FORM TI-12
12/97

WAPD-T-3231

CONF-990502--

RECEIVED
FEB 05 1999
OSTI

Dynamic and Static Error Analyses of Neutron Radiography Testing

H. Joo and S. S. Glickstein

DE-AC11-93PN38195

BETTIS ATOMIC POWER LABORATORY WEST MIFFLIN, PENNSYLVANIA 15122-0079

Operated for the U.S. Department of Energy
by WESTINGHOUSE ELECTRIC COMPANY,
a division of CBS Corporation

DISCLAIMER

DYNAMIC AND STATIC ERROR ANALYSES OF NEUTRON RADIOGRAPHY TESTING

H. Joo and S. S. Glickstein
Westinghouse Electric Company
Bettis Atomic Power laboratory

ABSTRACT

Neutron radiography systems are being used for real-time visualization of the dynamic behavior as well as time-averaged measurements of spatial vapor fraction distributions for two phase fluids. The data in the form of video images are typically recorded on videotape at 30 frames per second. Image analysis of the video pictures is used to extract time-dependent or time-averaged data. The determination of the average vapor fraction requires averaging of the logarithm of time-dependent intensity measurements of the neutron beam (gray scale distribution of the image) that passes through the fluid. This could be significantly different than averaging the intensity of the transmitted beam and then taking the logarithm of that term. This difference is termed the dynamic error (error in the time-averaged vapor fractions due to the inherent time-dependence of the measured data) and is separate from the static error (statistical sampling uncertainty). Detailed analyses of both sources of errors are discussed.

I. INTRODUCTION

A video-image analysis technique has been developed to extract average vapor fractions from real-time video-taped neutron attenuation data obtained at the Pennsylvania State University neutron radiography facility (References 1-4). This consists of measuring the gray level distribution throughout the flow region "illuminated" by the thermal neutron beam. In real-time television pictures, liquid regions appear dark (high neutron removal), and vapor appears light. The time-dependent brightness information (gray level data) is processed to produce a spatial distribution of time-averaged vapor fraction over the illuminated region of the conduit. The data reduction system was initially based on a time-averaging technique which can cause an error (dynamic error) that is related to fluctuations in the local density of the two-phase fluid. In a flow where there are no fluctuations in the fluid density during a unit counting interval, there still exist statistical uncertainties (static error) in measured variables. The main source of the static error is considered to be the neutron beam intensity and the gain of the neutron-image intensifier that converts a neutron image into a visible image. The dynamic error is related to the time-dependent fluctuations in the local composition of vapor-liquid mixtures. It results from the fact that the logarithm of the time-averaged intensity of the transmitted neutron beam ("Count-Mode Measure", Reference 5) is not equal to the time-averaged value of the logarithm of the intensity of the beam which is considered to be exact. An in-depth analysis of both the static and dynamic errors was conducted to help quantify the achievable errors and also to provide insight into the systematic errors associated with the neutron radiography technique developed for vapor fraction measurements.

II. STATIC ERROR IN VAPOR FRACTION MEASUREMENT

Consider a beam of neutrons impinging on a conduit containing a vapor-water mixture. If the change of the neutron intensity is approximated by an exponential attenuation, the vapor

fraction F(x,y) measured along the neutron beam direction at the point (x,y) on the surface of the two-phase flow regime is given (Reference 6) by

$$F(x,y) = \frac{1 - \dfrac{\ln\left[\dfrac{V(x,y)}{E(x,y)}\right]}{\ln\left[\dfrac{W(x,y)}{E(x,y)}\right]}}{1 - \dfrac{\mu_v}{\mu_w}}, \qquad \text{(A-1)}$$

V(x,y) = the intensity of the transmitted beam at (x,y) when the conduit is filled with a mixture of water and vapor,
W(x,y) = the beam intensity when the conduit is filled with water,
E(x,y) = the beam intensity when the conduit is empty,
μ_v = the effective attenuation coefficient of vapor, and
μ_w = the effective attenuation coefficient of water.

II.A. STATIC ERROR

Since the vapor fraction in Equation (A-1) is a function of the three measured variables, V(x,y), W(x,y) and E(x,y), the relation between the uncertainties of the variables and the uncertainty for the result, F(x,y), can be calculated by the second-power equation of the propagation of errors (References 7 and 8). If T(x,y) is the thickness of the attenuating medium at point (x,y), the relative error in the vapor fraction can be shown (Reference 9) as follows,

$$\frac{\Delta F(x,y)}{F(x,y)} = \frac{\sqrt{2}\,\dfrac{\Delta V(x,y)}{V(x,y)}}{\mu_w T(x,y)} \sqrt{1 - \frac{1}{\bar{F}} + \frac{1}{\bar{F}^2}}\,. \qquad \text{(A-2)}$$

where $\bar{F} = F(x,y)\,[1 - \mu_v/\mu_w]$. In Eq. (A-2), the term $\Delta V/V$ is the inherent statistical uncertainty of the intensity of the transmitted neutron beam at (x,y) when the conduit is filled with a mixture of water and vapor.

We can have some estimate of the sample variance if we were to repeat the measurement many times. Because we have only a single measurement, however, the sample variance cannot be calculated directly but must be estimated by analogy with an appropriate statistical model. Let us assume that detection of the transmitted neutrons is characterized by a Poisson process (References 10 and 11), which implies that

$$\frac{\Delta V(x,y)}{V(x,y)} = \frac{1}{\sqrt{N(x,y)}}, \qquad \text{(A-3)}$$

where N(x,y) is the number of counts measured by a unit detector element corresponding to a position (x,y) in the test device.

When a real-time video camera is used to record the intensity of transmitted neutrons, the final unit detector element is a small surface area which corresponds to a single video image pixel of the camera. Converting the detectable neutron intensity to a measurable signal, the number of counts at a steady-state condition measured during a unit counting interval is given by

$$N(x,y) = G_e\, t_o\, \Delta x \Delta y\, V(x,y), \qquad \text{(A-4)}$$

where

G_e = detector gain; number of counts of measurable signal per neutron interacting with the detector (counts/neutrons),
t_o = counting interval (sec),
$\Delta x\, \Delta y$ = surface area of unit detector element (cm^2), and
$V(x,y)$ = intensity of transmitted neutron beam (neutrons/cm^2/s).

II.B. Maximum Static Error

It can be shown (Reference 9) that the maximum static error in vapor fraction is given by the following equation:

$$\text{Max. } \Delta F(x,y) = \sqrt{\frac{2}{N_o(x,y)}}\ \frac{C_o}{R(x,y)}\ e^{R(x,y)/2}. \qquad \text{(A-5)}$$

where $N_o(x,y) = G_e\, t_o\, \Delta x \Delta y\, E(x,y)$, $C_o = \mu_w/(\mu_w - \mu_v)$, and $R(x,y) = \mu_w\, T(x,y)$. Under operating conditions using the Precise Optics neutron radiography camera at the Penn State University reactor facility, we have typical specifications for $N_o(x,y)$ given by the following parameters:

$G_e \approx 300$ counts/neutron (References 11 and 12)
Counting interval; $t_o = 1/30$ sec (for a single frame of real-time video image)
Detector element size; $\Delta x = \Delta y = 0.05$ cm (corresponding to a video pixel)
Source neutron intensity; $I_o = 2 \times 10^6$ neutrons/$cm^2 \cdot s$

The worst-case maximum static error in vapor fraction is evaluated as a function of the relative path thickness, R(x,y), using the limiting value of $C_o = 1.2$. Results are shown in Figure 1. The maximum static error occurs when the vapor fraction is zero. Also shown in Figure 1 is the static error when the vapor fraction is unity.

III. Dynamic Error Analysis

When a time-averaged vapor fraction is calculated, a time-averaged value of V(x,y) in Eq. (A-1) is frequently used. Therefore, it is necessary to evaluate the dynamic error associated with the neutron radiography data processing technique that utilizes the time-averaged V(x,y). The

dynamic error results from the fact that the time-averaged value of the logarithm, ln V(x,y), in Eq. (A-1) is not equal to the logarithm of the time-averaged intensity of the transmitted beam, V(x,y).

The time-averaged vapor fraction, $\overline{F_c}(x,y)$, calculated by the Count-Mode Measure with a time-averaged intensity of the transmitted beam, $\overline{V}(x,y)$, is given by

$$\overline{F_c}(x,y) = C_o \frac{\ln\left[\dfrac{\overline{V}(x,y)}{W(x,y)}\right]}{\ln\left[\dfrac{E(x,y)}{W(x,y)}\right]}, \qquad \text{(B-1)}$$

where $\overline{V}(x,y) = \dfrac{1}{\tau}\int_o^\tau V(x,y,t)dt$, τ = measurement time period, and other quantities, μ_v, μ_w, W(x,y) and E(x,y), are time-independent. It can be shown (Reference 9) that the dynamic error, $\Delta\overline{F}(x,y)$, can be written as

$$\Delta\overline{F}(x,y) = \overline{F_c}(x,y) - \overline{F}(x,y)$$

$$= C_1\left\{\ln\left[\frac{1}{n}\sum_{j=1}^{n} V_j(x,y)\right] - \ln\left[\prod_{j=1}^{n} V_j(x,y)\right]^{1/n}\right\}, \qquad \text{(B-2)}$$

where

$$C_1 = \frac{C_o}{\ln\left[\dfrac{E}{W}\right]}.$$

Eq. (B-2) indicates that whenever the intensity, V_j (x,y), of the transmitted beam at (x,y) during a time interval of $t_j \sim t_j + \Delta t$, is known for every time subinterval, the dynamic error can be determined by the difference of the logarithms of the two types of average values,

$$\frac{1}{n}\sum_{j=1}^{n} V_j(x,y) \text{ and } \left[\prod_{j=1}^{n} V_j(x,y)\right]^{1/n}.$$

III.A. Binomial Vapor Fractions

We are particularly interested in time-averaged vapor fractions of a two-phase flow simulated by an acrylic disc with holes (partial or full depth) in it. Such a configuration is applicable to experiments discussed in Reference 3. The time-dependent vapor (void) fractions are represented as a series of step changes between two values of $F(x,y,t)$, $F_1(x,y)$ and $F_2(x,y)$; that is, a binomial pattern.

Consider a case where $F_2(x,y) > F_1(x,y)$ and $F_2(x,y) = F_1(x,y) + \delta(x,y)$, where $\delta(x,y)$ is the magnitiude of the step change. Also defined are the intensities of the transmitted beam $V_1(x,y)$ and $V_2(x,y)$ corresponding to the vapor fractions $F_1(x,y)$ and $F_2(x,y)$, respectively. During a time period of τ, it is assumed that $V_1(x,y)$ is recorded at m subintervals and $V_2(x,y)$ is recorded (or measured) at (n-m) subintervals. It is also assumed that the time subinterval is sufficiently small so that the fluctuation in the measurement $V(x,y)$ within the subinterval is considered negligible. A fraction of the time period α is defined as

$$\alpha = m/n \quad \text{or} \quad 1 - \alpha = (n-m)/n.$$

Under such conditions, it can be shown (Reference 9) that the change of dynamic error (fractional error) with R(x,y) is given in Table 1. Similar results for changes of the dynamic error with α are given in Table 2. The values of α for the maximum dynamic error is given in Table 3 and the absolute dynamic error at specific conditions are shown in Table 4. Table 5 provides results for the change in dynamic error with respect to $\delta(x,y)$, and Table 6 shows the absolute dynamic error as a function of R(x,y).

Table 1. Change of Dynamic Error with R(x,y)

$\partial \Delta \bar{F}(x,y)/\partial R$

R (x,y)	$\delta = 0.5$, $\alpha = 0.5$	$\delta = 0.8$, $\alpha = 0.5$
0.1	0.0312	0.0799
0.5	0.0310	0.0784
1.0	0.0303	0.0740
2.0	0.0277	0.0601

Table 2. Change of Dynamic Error with α

$\partial \Delta \bar{F}(x,y)/\partial \alpha$

R(x,y)	$\delta = 0.5$, $\alpha = 0.5$	$\delta = 0.8$, $\alpha = 0.5$
0.1	0.0001	0.0004
0.5	0.0026	0.0105
1.0	0.0102	0.0401
2.0	0.0379	0.1360

Table 3. Values of α for Maximum Dynamic Error

R(x,y)	α for maximum dynamic error, α_m		
	$\delta = 0.2$	$\delta = 0.5$	$\delta = 0.8$
0.1	0.5017	0.5042	0.5067
0.5	0.5083	0.5208	0.5332
1.0	0.5167	0.5415	0.5660
2.0	0.5332	0.5820	0.6280

Table 4. Dynamic Error

R(x,y)	$\delta = 0.5$, $\alpha = 0.5$	$\delta = 0.8$, $\alpha = 0.5$
0.1	0.0031	0.0080
0.5	0.0156	0.0397
1.0	0.0309	0.0780
2.0	0.0601	0.1454

Table 5. Change of Dynamic Error with $\delta(x,y)$

R(x,y)	$\delta = 0.5$, $\alpha = 0.5$	$\delta = 0.8$, $\alpha = 0.5$
0.1	0.0125	0.0200
0.5	0.0622	0.0987
1.0	0.1225	0.1900
2.0	0.2311	0.3320

Table 6. Maximum Dynamic Error versus R(x,y)

R(x,y)	α_m	Maximum $\Delta\bar{F}$
0.1	0.5083	0.0125
0.5	0.5415	0.0623
1.0	0.5820	0.1233
1.5	0.6206	0.1819
2.0	0.6565	0.2372
3.0	0.7191	0.3358

III.B. Dynamic Error from Linear Vapor Fraction

We have conducted a dynamic error analysis in Section III.A utilizing a binomial pattern of vapor fraction distribution, which is considered to be an extreme case that can result in the most severe dynamic errors. Only the lowest and highest values of the vapor fraction were assumed present during a measurement period, precluding intermediate vapor fractions between the limits. As an intermediate case, we examined a condition where the vapor fraction at a spatial element tends to be smooth and continuous rather than abrupt and discontinuous (as a function of time). A simplistic, smooth and continuous fluctuation of vapor fraction as a function of time can be modeled by a linear function. A linear vapor fraction distribution during a measurement period and associated dynamic error were studied and details of the study are presented in Reference 9. The results are shown in Tables 7-9.

Table 7. Change of Dynamic Error with Flow Path Thickness (Linear Vapor Fraction Model)

	$\partial\Delta\bar{F}(x,y)/\partial R(x,y)$			
R(x,y)	δ=0.2	δ=0.5	δ=0.8	δ=1.0
0.1	0.00167	0.01042	0.0267	0.0417
0.5	0.00167	0.01040	0.0266	0.0414
1.0	0.00167	0.01035	0.0263	0.0407
2.0	0.00166	0.01016	0.0251	0.0379

Table 8. Change of Dynamic Error with $\delta(x,y)$ - Linear Model

	$\partial\Delta\bar{F}(x,y)/\partial\delta(x,y)$			
R(x,y)	δ=0.2	δ=0.5	δ=0.8	δ=1.0
0.1	0.0017	0.0042	0.0067	0.0083
0.5	0.0083	0.0208	0.0332	0.0415
1.0	0.0167	0.0415	0.0660	0.0820
2.0	0.0332	0.0820	0.1280	0.1565

Table 9. Dynamic Error versus Flow Path Thickness - Linear Model

R(x,y)	ΔF (x,y)			
	δ=0.2	δ=0.5	δ=0.8	δ=1.0
0.1	0.0002	0.0010	0.0027	0.0042
0.5	0.0008	0.0052	0.0133	0.0208
1.0	0.0017	0.0104	0.0265	0.0413
2.0	0.0033	0.0207	0.0522	0.0807

Relative to the binomial vapor fraction case the linear vapor fraction model results in smaller dynamic errors by a factor of three for a wide range of R(x,y) as illustrated in Figure 3.

IV. SUMMARY AND CONCLUSIONS

An analysis of both the static error and dynamic error was conducted to help quantify the achievable maximum errors and also to provide insight into the systematic errors associated with the neutron radiography technique developed for vapor fraction measurements for two-phase fluid flow.

The static error is a measure of the statistical uncertainty interval in the vapor fraction. It is determined by the propagation of uncertainty intervals of measured intensities of neutron beams. It has been found that the maximum static error occurs at zero vapor fraction and is slightly sensitive to the flow path thickness within the range of interest. For flow path thicknesses ranging from 0.3 cm to 1.3 cm, the maximum fractional error in vapor fraction is 0.02. This result is based on a neutron flux level of $2x10^6 n/cm^2/s$ using a Precise Optics camera. With increased source beam intensity the error can be reduced by a factor proportional to the square root of the gain in the source beam intensity.

The dynamic error in the vapor fraction is due to the inherent time-dependence of the measured data when the data is time-averaged by the Count-Mode measure. The dynamic error depends primarily upon and increases with the extent of the fluctuation in the local density of two-phase fluids and the flow path thickness. For the case where the flow path thickness is 0.22 cm, it has been found that the maximum possible dynamic error under the most extreme condition could be as large as 0.08 in vapor fractions. However, this number is a worst case upper limit and significantly larger than what was observed during an actual data acquisition process using the Exact Measure technique in the void fraction measurements of the acrylic discs. The majority of vapor fraction measurements involve less extreme conditions which result in smaller errors. For a less extreme case in which the fluctuation in vapor fractions was modeled as a linear function of time, the maximum dynamic error is approximately 0.03.

The Exact Measure technique minimizes the potential dynamic error that is caused by the Count-Mode measure. To do the Exact Measure technique, the logarithm of the intensity of the neutron beam obtained per video image must be taken before time-averaging the data.

References:

1. S. S. Glickstein, H. Joo and W. H. Vance, "Interpreting Neutron Radiographs Via Computer Simulation," Proceedings of the Fourth World Conference on Neutron Radiography, 761-770, May 1992.

2. S. S. Glickstein, W. H. Vance and H. Joo, "Void Fraction Measurements Using Neutron Radiography," Transaction of the ANS/ENS 1992 International Conference, November 1992; Nuc. Sci. & Eng., 121 153-161 (1995).

3. S. S. Glickstein, H. Joo, W. H. Vance and J. H. Murphy, "Void Fraction Measurements of Acrylic Discs Via Neutron Radiography," Transaction of the ANS 1994 Annual Meeting, June 1994.

4. S. S. Glickstein, J. H. Murphy and R. B. Hammond, "Void Fraction Measurements in a Steam Water Duct at Atmospheric Pressures Using Neutron Radiography," ASME Conference on Flow Visualization and Image Procesing of Multiphase Systems," August 1995.

5. T. J. Honan and R. T. Lahey, Jr., "The Measurement of Phase Separation in Wyes and Tees," NUREG/CR-0557, December 1978.

6. H. Joo and S. S. Glickstein, "A Scattering Probability Method for Vapor Fraction Measurements by Neutron Radiography," Third International Topical Meeting on Neutron Radiography, March 16-19, 1998.

7. S. J. Kline and F. A. McClintock, "Describing Uncertainties in Single Sample Experiments," Trans. ASME, January 1953.

8. G. F. Knoll, "Radiation Detection and Measurement," John Wiley & Sons, New York, 1979.

9 H. Joo and S. S. Glickstein, "Detailed Analyses of Dynamic and Static Errors in Neutron Radiography Testing," WAPD-TM 1637, Westinghouse Electric Company, Bettis Atomic Power Laboratory, January 1999

10. J. L. Bogdanoff and F. Kozin, "Probabilistic Models of Cumulative Damage," John Wiley & Sons, New York, 1985.

11. M. Verat, H. Rougeot and B. Driard, "Neutron Image Intensifier Tubes," Neutron Radiography by J. P. Barton and P. von der Hardt (eds.) 601-607, ECSC, EEC, EAEC, Brussels and Luxembourg, 1983.

12. D. E. Hughes, "The Development of Real Time Neutron Radiography at the Penn State Breazeale Reactor," M. S. Thesis, Pennsylvania State University, December 1986.

Figure 1

Maximum Static Error Versus Flow Path Thickness *

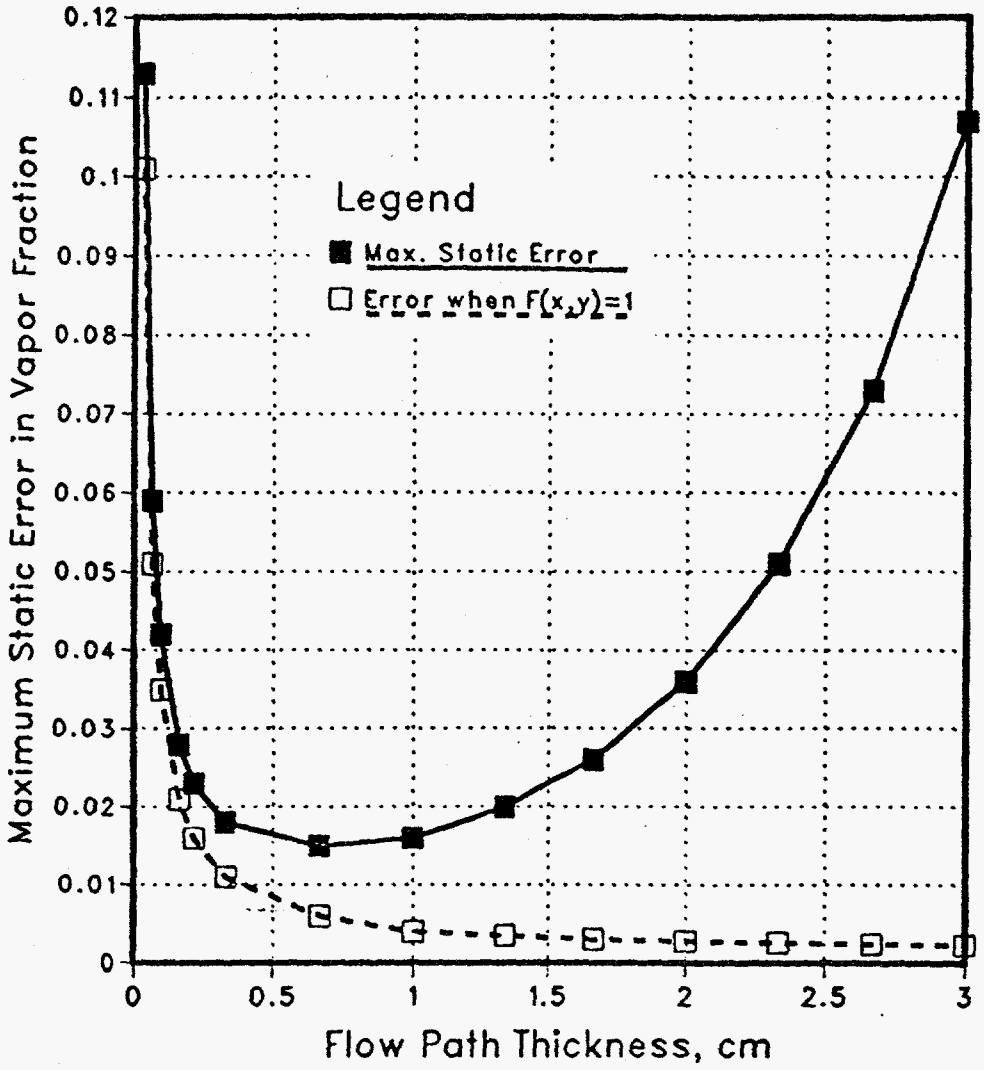

* The attenuation coefficient of water used was 3.0 cm^{-1}, and other data were based on specifications of the Penn State reactor facility. The maximum static error occurs when the vapor fraction becomes zero.

Figure 2

Dynamic Error in Void Fractions for an Acrylic Disc with Holes *

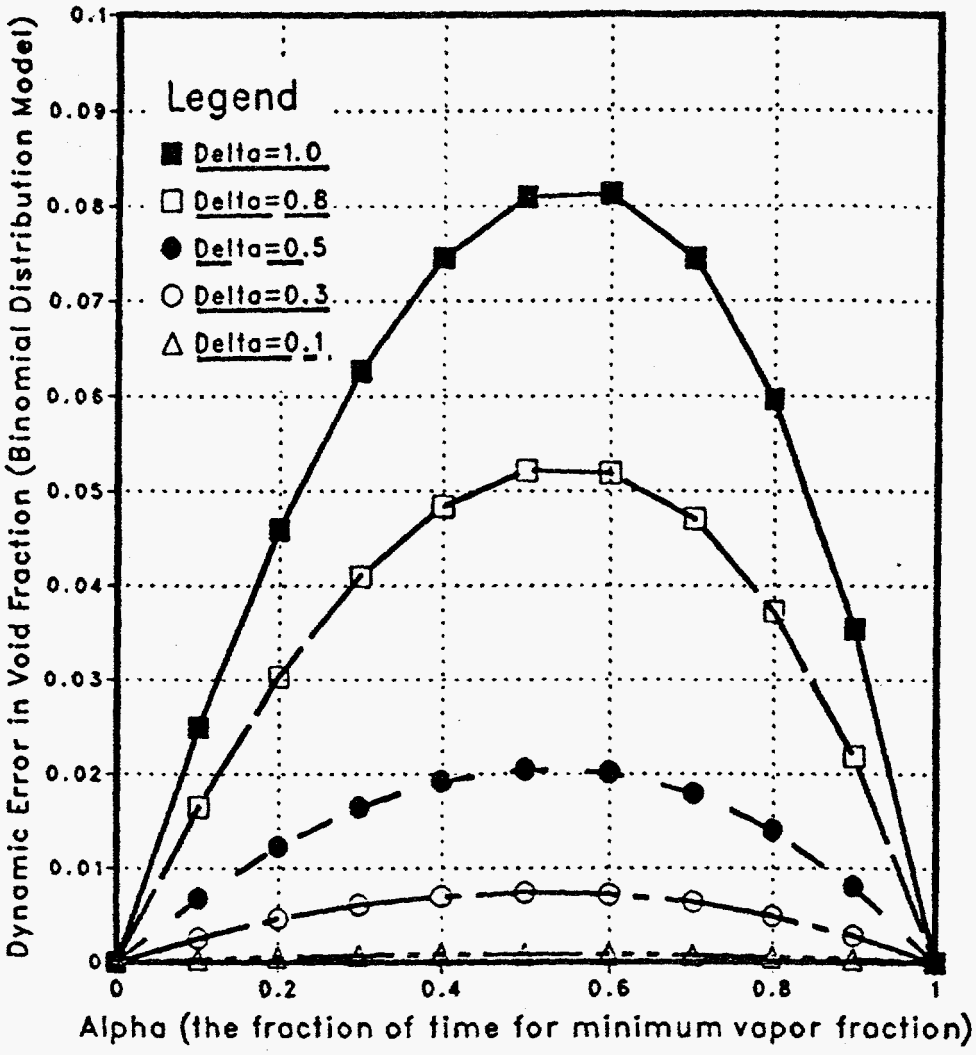

Delta = fluctuation in local void fractions during a measurement period
= maximum void fraction - minimum void fraction

* The attenuation coefficient of the disc = 3.0 cm^{-1}
Thickness of the disc = 0.22 cm

Figure 3

Maximum Dynamic Error Versus Flow Path Thickness *
(Vapor Fraction Patterns = Binomial Model and Linear Model)

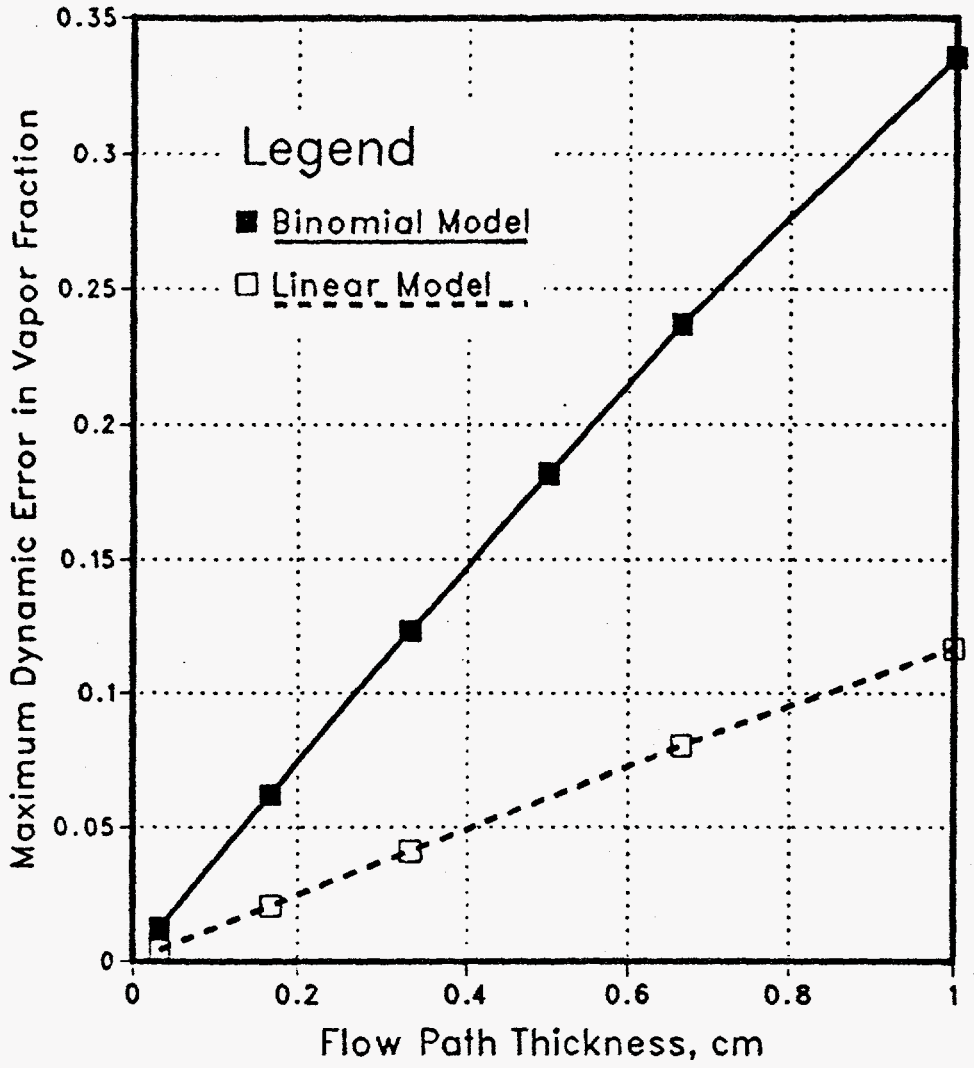

* The attenuation coefficients of water and vapor used are 3.0 cm^{-1} and 0.0 cm^{-1}, respectively. Optimum α values for the maximum error and δ=1.0 were used for the worst case.